DETECTION OF *CANDIDATUS* PHYTOPLASMA AURANTIFOLIA WITH A QUANTUM DOTS FRET-BASED BIOSENSOR

F. Rad[1,3], A. Mohsenifar[1,4], M. Tabatabaei[1,2], M.R. Safarnejad[1,5], F. Shahryari[2,4], H. Safarpour[1,3], A. Foroutan[6], M. Mardi[2], D. Davoudi[2] and M. Fotokian[3]

[1] *Nanosystems Research Team (NRT), Microbial Biotechnology and Biosafety, Agriculture Biotechnology Research Institute of Iran (ABRII), 31535-1897 Karaj, Iran*
[2] *Agriculture Biotechnology Research Institute of Iran (ABRII), 31535-1897 Karaj, Iran*
[3] *Shahed University, 3319118651 Tehran, Iran*
[4] *Tarbiat Modares University (TMU), 14155-4838 Tehran, Iran*
[5] *Iranian Research Institute of Plant Protection,19395-1454 Tehran, Iran*
[6] *Mazandaran University, 47416-95447 Sari, Iran*

SUMMARY

The witches' broom disease of lime (WBDL) supposedly caused by *Candidatus* Phytoplasma aurantifolia (*Ca.* P. aurantifolia) is the most devastating disease of lime in Oman and southern parts of Iran. The present study describes developing a quantum dot (QD)-based nano-biosensor for the highly sensitive detection of phytoplasma in infected trees. The immunodominant membrane protein (IMP) expressed in the surface of phytoplasma was selected as a target protein for construction of a specific binding antibody. The antibody (anti-IMP) was effectively conjugated to tioglicolic acid-modified cadmium-telluride quantum dots (CdTe-QDs) synthesized in an aqueous solution via electrostatic interaction. Dye (rhodamine) molecules were attached to the IMP, then, the donor-acceptor complexes (QDs-Ab-IMP-Rhodamine) were formed based on the antigen-antibody interaction. The mutual affinity of the antigen and the antibody brought the CdTe QDs and rhodamine together close enough to allow the fluorescence resonance energy transfer (FRET) to occur. The immunosensor constructed showed a high sensitivity and specificity of 100%, a detection limit of 5 *ca.* P. aurantifolia/µl, and acceptable stability, so it could be used for detection with consistent results.

Key words: biosensing; detection, *Candidatus* Phytoplasma aurantifolia, quantum dots (QDs), FRET, immunodominant membrane protein (IMP).

INTRODUCTION

Over the past decade, there has been a growing attention towards the various applications of nanobiothechnology. More specifically, nanoparticles due to their unique features including size-dependent, bright and extremely stable emissions have attracted a great deal of attention. One of the most promising nanomaterials are quantum dots (QDs) which have been widely used in a broad range of bio-related applications, such as imaging, cell tracking/trafficking and multiplexed biosensors used for disease diagnosis (Zhang *et al.*, 2010). In-time detection of pathogenic agents has always posed serious challenges and as a result, it is becoming increasingly difficult to ignore the necessity to apply novel tools such as QDs for rapid, accurate, and cost-effective detection purposes.

Among the plant pathogens, *Candidatus* Phytoplasma aurantifolia (*Ca.* P. aurantifolia), the causal agent of the witches' broom disease of lime trees (generally referred to as WBDL) (Zreik *et al.*, 1995), is regarded highly critical in some parts of the world. The disease was first observed in Oman followed by its catastrophic incidence in Iran (Bové, 1986; Bové *et al.*, 2000). The symptoms include yellowing, deformation, weakening and stunting of the plants which, eventually, lead to their death (Zamharir *et al.*, 2011). The disease has already caused the eradication of thousands of hectares of WBDL-affected trees impinging on the livelihood of rural communities in the affected areas.

Currently, the detection methods used for *Ca.* P. aurantifolia have some drawbacks limiting their straightforward application. For instance, serological methods are not sensitive enough for the detection of low amounts of the pathogen at the initial stages of infection (Lee *et al.*, 1998). On the other hand, DNA based-methods are not able to discriminate live from dead pathogens. DNA hybridization depends on radioactive and/or non-radioactive probes which may not be readily available, are costly and lengthen the detection time. To overcome these obstacles and provide more sensitive tools for establishing the presence of phytoplasmas in the plants, alternative approaches such as the use of bio-nanosensors should be considered.

Since the introduction of biocompatible QDs, the number of biotechnological applications reported for these versatile materials has grown rapidly. Many appli-

Corresponding author: M. Tabatabaei; M.R. Safarnejad
Fax: +98.2612704539; +98.2122403691
E-mail: meisam_tab@yahoo.com; safarnejad@iripp.ir

cations have focused on using QDs as protein- or DNA-conjugated fluorometric labels for cellular imaging, optical bar-coding, and immunoassays (Medintz *et al.*, 2003). QDs have a number of unique optical properties that are advantageous for developing bio-nanosensors based on the fluorescence resonance energy transfer (FRET) phenomenon (Algar and Krull, 2007). First, the synthesis of QDs is a relatively simple process and once synthesized, they have a relatively long shelf life. Moreover, minor modifications to the synthesis methods allow for a wide range of variations in the dot size and resultant optical properties. On the other hand, QDs were proven to be effective FRET donors due to their broad excitation spectra and tunable, narrow and symmetric photoemission (Youn *et al.*, 1995). Therefore, they could enhance FRET as an effective technique in molecular binding studies, protein conformation change, and biological assays. One of the most important significance of the combination of QDs and FRET system is their application as the QD-FRET-based biosensors which can be used for designing biomolecular detection systems. More specifically, they are applicable to pathogen detection in the samples of interest.

FRET efficiency (E) is strongly dependent on the donor-acceptor distance (r). Thus, it is important to reduce the "r" value to achieve higher E (hence sensitivity), i.e. the fluorescence emission spectrum of the donor must overlap the absorption spectrum of the acceptor. The emission spectra of QDs are narrow and symmetric, which greatly reduces the overlap between the emission spectra of donor and acceptor and avoids the mutual signal interference (Algar *et al.*, 2010). As a donor, QDs have broad excitation spectra, and there are many excitation wavelengths which can be used to avoid the direct excitation of the acceptor (Algar *et al.*, 2010). In addition, QDs have high photo-bleaching threshold and good chemical stability, which can greatly improve detection sensitivity and limits.

QD-based FRET biosensors have been widely used in immunoassay (Frasco and Chaniotakis, 2009; Ho *et al.*, 2009), biomedical sensors (Shi *et al.*, 2007; Tang *et al.*, 2008; Kim *et al.*, 2009), detection of protein (Algar and Krull, 2008; Liu *et al.*, 2008), and intermolecular binding assays (Goldman *et al.*, 2002a, 2002b; Goldman *et al.*, 2005; Gupta *et al.*, 2005; Zhang and Johnson, 2006). The main objective of the present study was to develop a specific and sensitive FRET-based QD-antibody biosensor for the rapid, accurate, and cost-effective detection of *Ca.* P. aurantifolia.

MATERIALS AND METHODS

Sampling. Throughout the present study, an infected specimen of Mexican lime grown in a greenhouse of the Agricultural Biotechnology Research Institute of Iran (ABRII) was used as a source of phytoplasma for isolation of IMP gene and subsequent analysis. This sample was previously collected from the Rodan area of the Hormozgan province. As a control, healthy Mexican lime plants grown under similar conditions were used. Samples were obtained from the midrib tissues and used for both DNA extraction and extract preparation. For evaluating the sensitivity of nanobiosensor against another phytoplasmas, infected samples of almond, alfalfa and sesame were gathered from the field in spring of 2011. The almond specimens were from infected orchards of the Birjand rarea (south Khorasan province), whereas infected sesame and alfalfa samples were kindly provided by Mr. Esmailzadeh from farms around the city of Yazd. For the nanobiosensor assay, leaf midrib tissues were crushed in Tris-HCl buffer, pH 7.1 (at the ratio of 1 g leaf: 300 µl buffer) and the extract obtained was used in the assay.

DNA extraction and phytoplasma infection detection. Total DNA was extracted from healthy and infected lime plants as described by Zhang *et al.* (1998). The *Ca.* P. aurantifolia infection was confirmed by nested PCR as described by Zamharir *et al.* (2011).

Cloning immunodominant membrane protein (IMP) gene. The immunodominant membrane protein (IMP) expressed at the phytoplasma surface was selected as a target protein for the construction of a specific binding antibody. The IMP gene (519 bp) was amplified using the PCR primers IMP28F/IMP28R (Table 1). Amplification products were recovered using a gel extraction kit (Roche, Germany) and cloned into a pTZ57R/T vector using InsT/Aclone™ PCR product cloning kit (Fermentas, Lithuania) following the manufacturer's instructions. Plasmid DNA was extracted from individual clones and purified using the high pure isolation kit (Roche, Germany) and custom sequenced

Table 1. Sequences of the primers used in this study.

Primer name	Sequence	Reference
IMP28F	5′ CAACGTCGACAAAATCACAAAGAAAATTTTTTAC 3′	This study
IMP28R	5′ CAACGCGGCCGCTTATGATAATTTTAAATCTG 3′	This study
IMP3-F	5' AGTTGGTGTGTTAGCATCTTT 3′	Askari *et al.*, 2011
IMP3-R	5' CTACTCTTTGTTTTCCACTT 3′	Askari *et al.*, 2011

in both directions (Macrogen, South Korea). Sequences were aligned and compared with phytoplasma sequences from GenBank using the BLAST search facility at the NCBI and the vectors carrying the right amplicons were selected.

Antigen preparation. The IMP coding region was cloned into the bacterial expression pET-28a vector and transformed into *E. coli* BL21 (DE3) competent cells (Fermentas, Lithuania). The expression and purification of the recombinant IMP from bacterial cultures was done as described by Shahryari *et al*. (2010). Recombinant proteins were purified by a Ni-agarose column (Qiagen, Germany). Protein concentration was measured using the Micro BCA kit (Pierce, UK). Protein analysis was performed using SDS-PAGE gels as described by Shahryari *et al.* (2010). The IMP obtained was then used for antibody preparation.

Immunization. Two 2-month-old females of New Zealand white rabbit were injected intramuscularly with 100 µg purified recombinant IMP diluted by an identical volume of Freund`s adjuvant. Serum was collected and antibodies were separated and purified with a mini spin column kit (AbD Serotec, UK). The titration was done by an indirect ELISA, as described by Shahryari *et al.* (2011).

CdTe quantum dots preparation. Tellurium powder (99.9%), cadmium chloride ($CdCl_2$, 99.9%), and thioglycolic acid (TGA, 98%) were purchased from Tianjin Chemical Reagents Company (China). Water-soluble CdTe QDs were synthesized by using 5 mM of $CdCl_2$-2.5 H_2O dissolved in 110 ml distilled water, followed by the addition of 12 mM TGA while stirring. pH was adjusted to 11 by drop-wise addition of 1 M NaOH solution. The solution was then placed in a three-necked flask and purged by N_2 for 30 min. Then, 2.5 mM of oxygen-free NaHTe solution, freshly prepared from tellurium powder and sodium borohydrate ($NaBH_4$, molar rate of 1:2) in water at 0°C, was injected into the three-necked flask while stirring. Finally, the resultant mixture was refluxed at 100°C for 4 h.

Bioconjugation of CdTe QDs with antibodies. A hundred µl of QDs (2 mg/ml) and 50 µl of the purified IMP antibodies (5 mg/ml) were mixed (pH 7.4). Then 150 µl of the freshly prepared 4.2 mg/ml 1-ethyl-3-(3 dimethylaminopropyl)-carbodiimide EDC (44 mM in borate buffer) was added to the mixture. The samples were incubated for 2 h at room temperature under shaking in the dark and stored at 4°C overnight. The overnight QDs-labelled antibodies were then centrifuged at 20,000 g for 20 min. The upper phase containing QDs-antibody conjugates was decanted and diluted by 1.5 ml Tris-HCl, then 0.5 ml of 50 mM Tris-HCl containing 1% BSA were added. Finally, the QDs-labelled antibodies were dispersed in Tris-HCl and stored at 4°C until use.

Conjugation of IMP with rhodamine as a quencher. In order to conjugate the IMP with rhodamine, first 360 µl of glutaraldehyde 10% (100 g/l) were gently added to 100 µl IMP (5 µg/ml). Subsequently, 2 µl of dinitropry-din was added while stirring and mixed for 30 min. In the next step, 1 mg of $NaBH_4$ was added and the mixture was stored for 1 h at room temperature. IMP-GLA conjugates were separated from the excess GLA via dialysis using Tris-HCl 50 mM for 24 h. Rhodamine 123 was used for conjugation to IMP-GLA, to this aim rhodamine solution (3 mg rhodamine/5 ml ddH_2O) was added to the dialyzed IMP-GLA solution. Finally, the rhodamine-GLA-IMP conjugates were separated from free rhodamine by dialysis as explained earlier.

Fluorometry instrumentation. Fluorescence spectra were obtained with a Shimadzu 1501 ultraviolet-visible spectrophotometer (Shimadzu, Japan). The fluorometer was operated at the excitation wavelength of CdTe QDs at 328 nm. The emission spectra were adjusted at between 540 and 640 nm to cover the emission range of the rhodamine (quencher) (580 to 600 nm).

Kit construction and evaluation. The constructed kit consisted of: (i) rhodamine-antigen (IMP) solution, (ii) QDs-labeled antibodies and, (iii) Tris-HCl buffer. The test was conducted by first adding 3 ml of the Tris-HCl buffer into the fluorometer cell. Then, 50 µl of the rhodamine-antigen solution was added followed by an addition of 50 µl of the QDs-labelled antibody solution. The baseline curve was then obtained for revealing the baseline emission of rhodamine quenching the emission caused by the QDs. At the detection stage, as mentioned earlier the midribs obtained from suspicious leaves (0.1-0.5 mm thick) were crushed in Tris-HCl buffer (1 g plant material/300 µl buffer). Ten µl of the prepared extract were then added to the same fluorometer cell and the second curve was obtained. If no or negligible baseline shift (based on the shift associated with the detection limit) was observed (negative), the sample was marked as *Ca*. P. aurantifoliae-free but a baseline downward shift or decline (positive) would reveal that the sample contained the pathogenic agents.

Consistency and specificity. In order to determine the consistency of the constructed QD FRET-based biosensor kit, an artificially contaminated sample was tested eight times in triplicate. The sample preparation was optimized and the final sample used was prepared by diluting 10 µl IMP 3500 µg/ml to the final concentration of 0.1 µg IMP/ml Tris-HCl buffer. Moreover, eight IMP-free samples were tested each in triplicate as

well. In addition, the specificity of the nanobiosensor for the detection of WBDL was analyzed using other important citrus diseases such as greening, bacterial canker and tristeza. Beside that, the nanobiosensor was also evaluated for detection of other phytoplasmas such as those infecting sesame, alfalfa, and almond. The baseline shift (decline) associated with the determined detection limit was used as a criterion to decide whether a sample was WBD-contaminated.

Stability. Fourier transform infrared (FT-IR) spectroscopy analysis was used to investigate the stability of the existing chemical bonds such as those between the QDs and the antibody molecules as well as those between rhodamine and antigen. To this aim, 150 µl of each QDs, QD-Ab and rhodamine-antigen were freeze-dried then used to make a tablet for FT-IR analysis with Nicolet IR100 FT-IR (Madison, USA).

Detection limit determination. Real-time PCR was used to determine the detection limit of the constructed bio-nanosensor. To achieve that, the pTZ57R/T vector harboring the IMP gene was used for the production of standard serial dilutions. Concentration of the purified plasmid sample was quantified using a spectrophotometer and converted to the gene copy number using the following equation (Whelan *et al.*, 2003):

$$\text{IMP gene copy number} = \frac{6.023 \times 10^{23}\ (\text{copies mol}^{-1}) \times \textit{DNA amount}\ (\text{g µl}^{-1})}{\textit{DNA length}\ (\text{bp}) \times 660\ (\text{gmol}^{-1}\text{bp}^{-1})}$$

To construct the standards, the artificial template was diluted to a final concentration of 10^7 to 10^1 IMP gene copies/µl sterile water. The standard dilutions of the cloned IMP gene were then used to establish a calibration curve by plotting the Ct, obtained by a 40 cycle real-time PCR, versus the log10 of the IMP gene copy number [log10 (copy number)]. Each calibration standard was tested in triplicate in three different runs. Threshold detection levels, Cts and the standard curves were calculated automatically by the Bio-Rad iCycler software, version 3.06070.

More specifically, the experiment was conducted using a specific primer pair IMP3-F/IMP3-R that amplifies a 158-bp DNA fragment of the IMP gene of *Ca.* P. aurantifolia (Table 1) (Askari *et al.*, 2011). Real-time PCR was conducted in 96-well optical reaction plates using the BioRad iCycler real-time PCR detection system (Biorad, USA). A 20 ml reaction mixture containing 1 µl of DNA template (20 ng DNA/µl), 0.2 µM of each primer, 10 µl of the iQ™ SYBR green supermix (Biorad, USA) and 7 µl of double distilled water was pipetted in each well. Control samples in each run included DNA from healthy lime tissues and water instead of the template DNA. Each sample was run in triplicates. Amplification conditions were: (i) incubation step at 94°C for 10 min, (ii) DNA amplification for 40 cycles of 94°C for 15 sec, 56°C for 30 sec, 72°C for 30 sec and a final extension at 72°C for 5 min. A melting curve temperature profile was obtained by heating the reaction from 50°C to 95°C with the ramp rate of 0.05°C per second to obtain the fluorescence measurements minimizing interference from primer-dimer or other non-specific amplification products. Product identity was confirmed using BioRad iCycler software, version 3.06070 (Biorad, USA) and by electrophoresis in 2% agarose gel. The threshold cycles (Ct) were calculated by plotting normalised fluorescence (ΔRn) in relation to the cycle number.

Finally, one extract obtained from a selected contaminated sample exhibiting severe symptoms of WBDL was prepared and its IMP gene copy number was measured as explained above. Serial dilutions ranging from 10^6 to 1 IMP gene copy number/µl were then prepared and tested by the constructed QD FRET-based biosensor kit to determine its detection limit. The baseline shift (decline) associated with the determined detection limit was used as a criterion for deciding whether a sample was WBD-contaminated.

Real sample examination. In order to investigate the kit's performance when real samples were used, 27 samples were prepared, 19 of which were contaminated and 8 pathogen-free, and tested by the constructed bio-nanosensor system.

RESULTS AND DISCUSSION

This report describes the application of luminescent semiconductor nanocrystals or quantum dots (QDs) coupled with FRET analysis as an accurate, cost-effective, and rapid immunoassay technique for WBDL. First, the IMP gene of 519-bp coding the pathogenic protein of the phytoplasma agent was amplified using the IMP28F/IMP28R primer set which confirmed that the phytoplasma isolates obtained were associated with the causal agent of WBDL. Database alignment of the sequences obtained revealed a 100% homology with *Ca.* P. aurantifolia sequences from database. The digested IMP gene from the pTZ57R/T vector was then cloned in the pET-28a vector and transferred into the competent cells. This resulted in the successful expression and production of the recombinant IMP which was then purified and its molecular weight was measured on a SDS PAGE gel at 19.7 kDa (Fig. 1).

The purified IMP with a known density was injected intramuscularly into two test rabbits and 6 weeks later, as determined by ELISA, an antiserum was recovered with a titer exceeding 1:100,000. The synthesized CdTe QDs were surface-modified with TGA and their mean particle diameter was measured at 8.2 nm. The purified

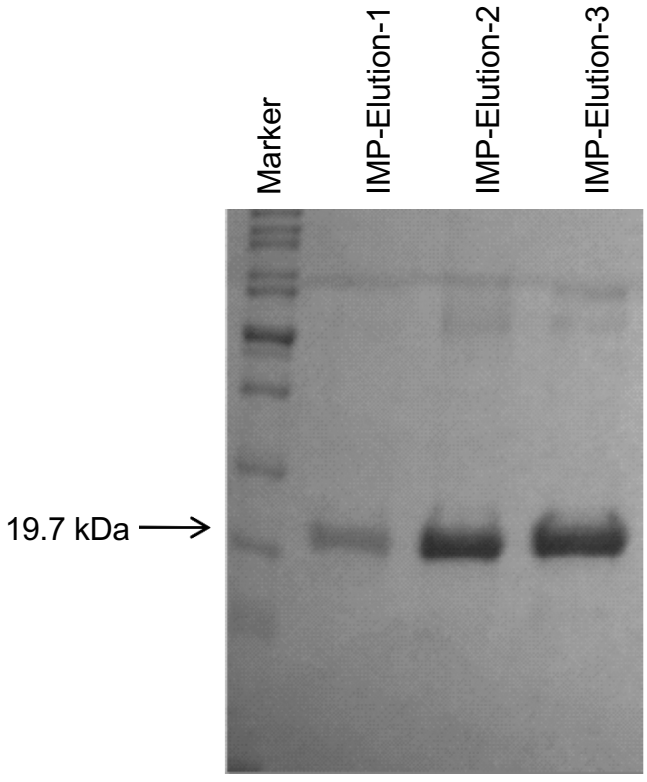

Fig. 1. SDS-PAGE gel showing the intensity of the IMP produced at different elution steps.

antibodied were immobilized on the prepared TGA-modified CdTe QDs. This was achieved due to the hydrophilic nature of the QDs leading to the attraction of IgGs onto their surfaces (Zhou and Ghosh, 2006). The Ab-QDs conjugates showed the maximum fluorescence radiation at approximately 545 nm. Concurrently, the IMP was successfully conjugated to rhodamine using the 24 free amine groups (lysine) of IMP linked to GLA. The two conjugates i.e. Ab-QDs and rhodamine-IMP were further conjugated based on the antibody-antigen interaction phenomenon. A fluorescence emission wavelength of the Ab-QDs of 410 AU was observed, however, the emission spectrum of the solution showed an upward shift peaking at 594 AU when the rhodamine-IMP/Ab-QD conjugates were investigated (Fig. 2). This was due to the loss of quenching effect of rhodamine on QD.

In principle, the antibody-antigen attachment is not of a robust type due to the non-covalent nature of the interactions (bonds) involved (Safarnejad *et al.*, 2011). This fact was exploited in developing the detection basis, since when a sample containing free IMP of phytoplasma origin was added to the solution (rhodamine-IMP/Ab-QD conjugates), the Rhodamine-IMP domain was replaced by the free IMP based on the concentration of the free IMP in the suspicious sample. This led to a downward shift of the fluorimeteric curve in comparison with the curve previously obtained for the rhodamine-IMP/Ab-QD conjugates. This could be explained through the optical quenching mechanism of the QD-antibody domain by the rhodamine-antigen domain based on the Forster dipole–dipole interaction model (Zhou and Ghosh, 2006). In other words, the inorganic dye, i.e. rhodamine (a fluorescence acceptor) conjugated to the antigen (IMP), occupied the peptide-binding pocket of the antibody, i.e. anti-IMP polyclonal antibody, resulting in a 3-fold FRET signal. Therefore, when free IMP derived from the pathogenic agent was added, it displaced the rhodamine-IMP domain in the rhodamine-IMP/Ab-QD conjugates, resulting in a decrease of fluorescence emission by displaced rhodamine-IMP whicc therefore was not excited anymore by QD emission (FRET) (Fig. 3). More specifically, the higher the concentration of the free IMP, the more the distribution of rhodamine-IMP domain/free IMP on the surface of the antibody molecules would shift in favour of the free IMP. In other words, a higher free native IMP concentration in the infected sample is translated into the fluorimeter curves obtained, peaking at lower photoluminescence (PL) intensity.

FT-IR spectra was used to reveal the stability of the constructs i.e. TGA-surface modified CdTe QDs, QD-Ab, and rhodamine-IMP conjugates (Fig. 4). Basically, FT-IR offers quantitative and qualitative analyses for organic and inorganic samples. This technique identifies the chemical bonds in a molecule by producing an infrared absorption spectrum. The spectra produce a profile of the sample, a distinctive molecular fingerprint that can be used to easily screen and scan samples for many different components. The peak obtained at 1900 cm^{-1} for QDs (Fig. 4), should be coincident with carbonyl stretching vibration, indicating that the CdTe QDs were successfully bound to the carboxylic acid functional group of TGA. The same peak (1900 cm^{-1})

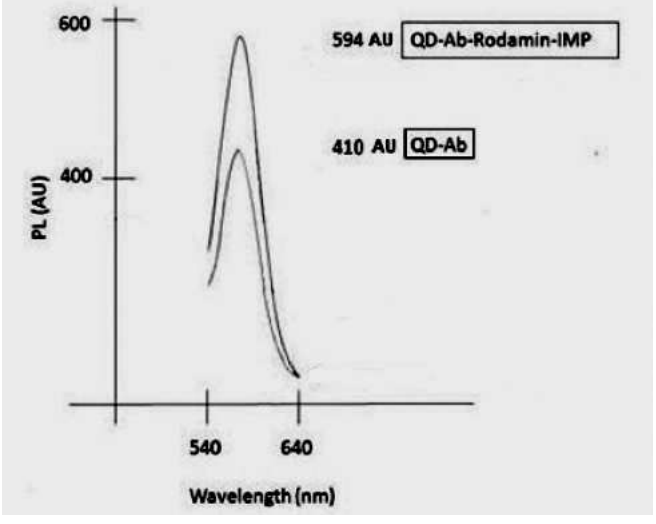

Fig. 2. The fluorometric peak of Ab-QDs conjugates and the QD-Ab-IMP-rhodamine complex.

Table 2. Threshold cycle (Ct) values and IMP gene copy numbers/µl lime midribs extract.

Serial Dilution (IMP gene copy number/µl)[a]	Threshold Cycle (Ct)
Standard 10^7	16.11
Standard 10^6	19.23
Standard 10^5	22.21
Standard 10^4	25.98
Standard 10^3	29.96
Standard 10^2	33.36
Standard 10^1	35.47
Healthy lime	-[b]
DNA free control (Water)	-[b]

[a] IMP gene copy number/µl = Number of phytoplasmas/µl
[b] No amplification

Table 3. Determination of the detection limit of the nanobiosensor.

IMP gene copy number/µl [a]	First run[b] (AU)	Second run[c] (AU)	Change
10^6	602	415	- 187
10^5	590	419	- 171
10^4	587	441	- 146
10^3	590	470	-120
10^2	589	493	- 96
10^1	580	512	- 68
5	594	554	- 40[d]
1	590	579	- 11

[a]IMP gene copy number/µl = Number of phytoplasmas/µl (serial dilutions prepared using a sample first analyzed by real time PCR)
[b]First run at 580 nm [buffer + (QDs-Ab) + (rhodamine-IMP)]
[c]Second run at 580 nm [buffer + (QDs-Ab) + (rhodamine-IMP) + sample]
[d]The baseline shift (- 40 AU) associated with the determined detection limit (5 phytoplasma/µl) has been used as a criterion to decide whether a sample is WBD-contaminated.

was observed for QD-Ab, however, it resulted from the –CO-NH mode or, in other words, the contributions of C-N stretching vibration and N-H bending vibration in the CdTe QDs and the antibody molecules, respectively. Moreover, the peak obtained at 1800 cm^{-1} for the rhodamine-IMP conjugates (Fig. 4), should be coincident with the amine stretching vibration. This indicated that amine groups of rhodamine were successfully bound to the aldehyde functional group (C-HO) of glutaraldehyde. The obtained results were successfully reproduced over the course of time. Therefore, the overall FT-IR analyses of the constructed conjugates revealed their stability.

In addition, the detection limit of the constructed kit was determined by real time-PCR. To determine the phytoplasma population in infected limes, real time-

Table 4. Analysis of plant materials with nanobiosensor.

Plant samples	First run[a] (AU)	Second run[b] (AU)	Change[c]
Lime Witches` broom (positive control)	641.7	548.7 [d]	- 93
Healthy lime (negative control)	687.3	686.7	± 0.6
Bacterial citrus canker	696.5[c]	709.5	± 13
Citrus tristeza	679.5	698.5	± 19
Citrus uanglongbing	668.5	656	± 12.5
Alfalfa witches` broom	646	668.5	± 22.5
Almond witches` broom	700	709.5	± 9.5
Sesame witches` broom	685.8	698.5	± 12.7

[a]First run at 580 nm [buffer + (QDs-Ab) + (rhodamine-IMP)]
[b]Second run at 580 nm [buffer + (QDs-Ab) + (rhodamine-IMP) + sample]
[c]The baseline shift (- 40 AU) associated with the determined detection limit (5 phytoplasma/µl) has been used as a criterion to decide whether a sample is WBD-contaminated.
[d]Each measurement is an average over three replicates

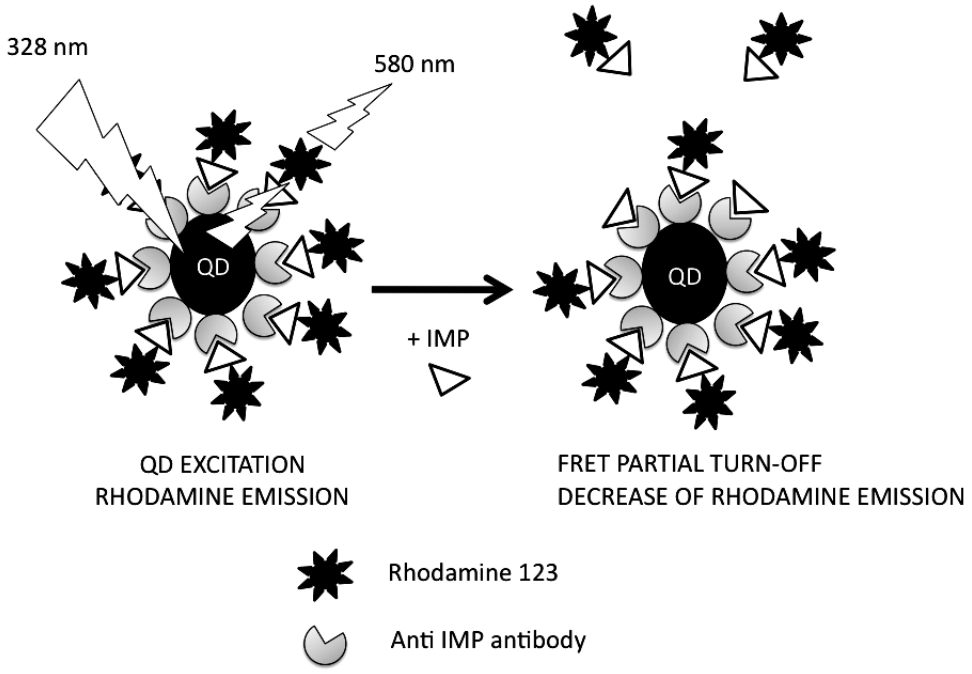

Fig. 3. Schematic representation of the functional mechanism of the CdTe QD-Ab nanosensor. Each QD (emission wavelength, 560 nm) is surrounded by an average of 24 Ab molecules, however, only a single Ab is shown in the picture for simplicity. Formation of QD-Ab-IMP-rhodamine complex (maximum absorption at *ca*. 594 nm) results in the quenching of the QD emission. Added IMP displaces rhodamine-IMP conjugates from the sensor assembly, resulting in an increase in the direct QD emission.

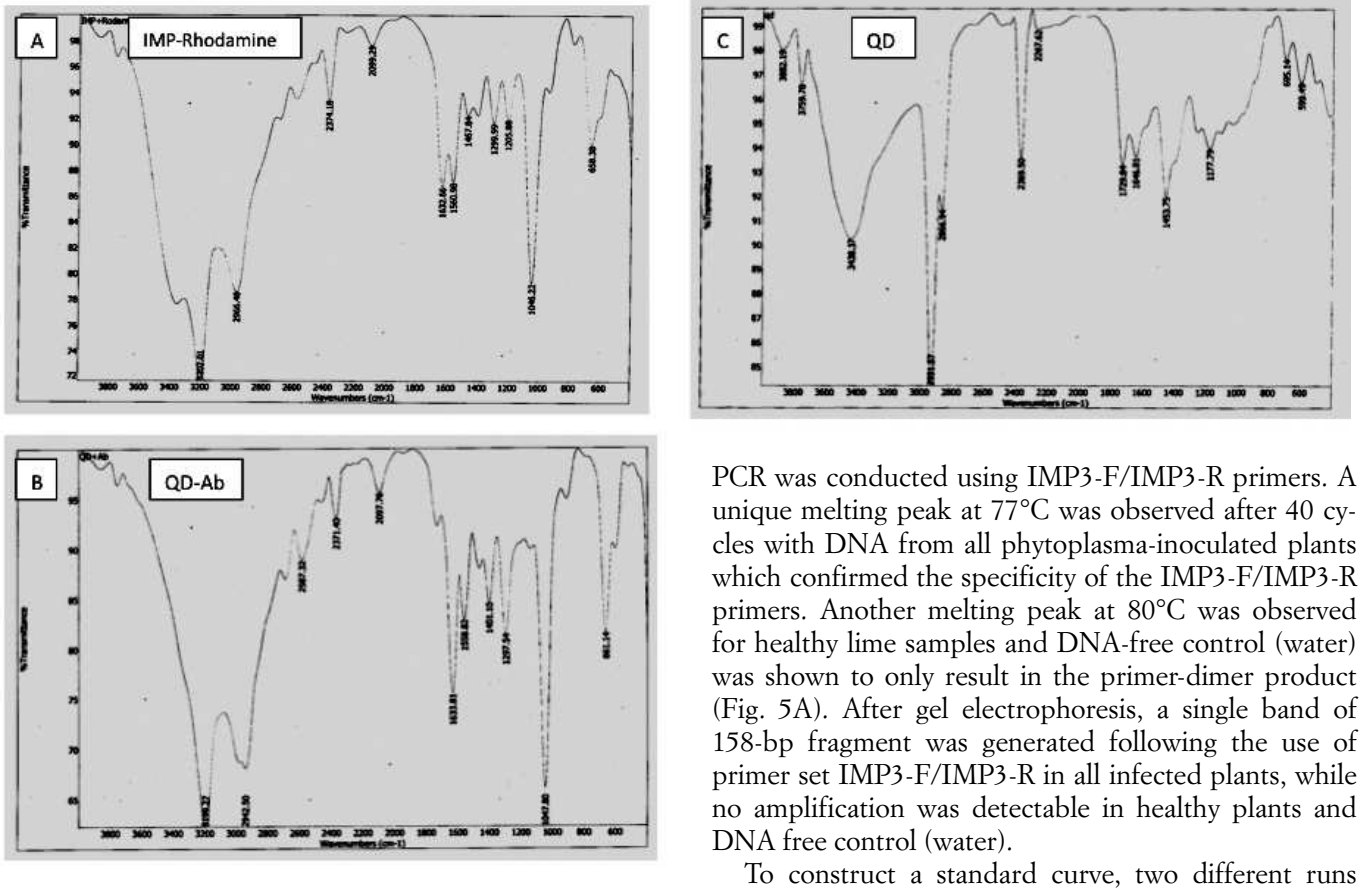

Fig. 4. FT-IR spectra of A, the rhodamine-IMP conjugate; B, the Ab-QDs conjugate and, C, CdSe QDs.

PCR was conducted using IMP3-F/IMP3-R primers. A unique melting peak at 77°C was observed after 40 cycles with DNA from all phytoplasma-inoculated plants which confirmed the specificity of the IMP3-F/IMP3-R primers. Another melting peak at 80°C was observed for healthy lime samples and DNA-free control (water) was shown to only result in the primer-dimer product (Fig. 5A). After gel electrophoresis, a single band of 158-bp fragment was generated following the use of primer set IMP3-F/IMP3-R in all infected plants, while no amplification was detectable in healthy plants and DNA free control (water).

To construct a standard curve, two different runs were conducted using 10^1 to 10^7 IMP gene copy number dilutions. Both runs showed a high linear depend-

ence between the two variables, with correlation coefficients of about 0.99. A statistical analysis also confirmed the linearity between the Ct values versus the logarithm of the copy number of the IMP gene; 10^1 to 10^7 (Fig. 5B, Table 2). The threshold cycle (Ct) in the real-time PCR reactions was used as a criterion for quantifying the phytoplasma number in a selected contaminated plant sample exhibiting severe symptoms of WBDL. Then, the serial dilutions ranging from 10^6 to 1 IMP gene copy number/µl were prepared and tested by the constructed QD FRET-based biosensor kit. Given the results obtained, the detection limit was measured at 5 *Ca.* P. aurantifolia/µl fresh leaf extract sample (Table 3).

The consistency of the constructed bio-nanosensor kit was found to be as high as 100%. The results obtained from analysis of infected citrus plant samples by *Ca.* Liberibacter asiaticus, *Xanthomonas citri* f. sp. *citri* and *Citrus tristeza virus* (CTV), the agents of citrus greening, bacterial canker and tristeza, respectively, revealed no cross reaction (Table 4). The complementary results gained by analyzing three other phytoplasma diseases such as those affecting sesame, alfalfa and almond indicated also no cross reaction (Table 4). The baseline shift (-40 AU) associated with the determined detection limit (5 phytoplasma/µl) was used as a criterion to decide whether a sample is WBD-contaminated. The baseline shifts i.e. upward or downward, were less than 40 AU in the case of all the other phytoplasma species tested.

Finally, when 27 samples (19 WBDL-infected and, 8 healthy lime samples) were tested, the constructed bio-nanosensor performed with a complete accuracy and managed to efficiently detect the samples carrying the phytoplasma agents (Table 5).

Till the year 2008 and in Iran alone, WBDL claimed the death of over half a million trees and the disease continued to spread until recently (WBDLN, 2010). Sadly, in 2009, the causal agent of the disease expanded its territory to other plants such as grapefruit and it is anticipated that it will pose a serious threat to the other horticultural products in Iran and elsewhere. The homogenous antigen-antibody assay technique and the FRET-based nano-biosensor constructed as described in this paper has several advantages over the conventional detection methods, including significantly higher sensitivity and simplicity in the detection of the pathogen even at the very early stages of the infection within the incubation period.

Table 5. Analysis of samples (20 WBDL-infected and 8 healthy lime samples) with the constructed bio-nanosensor.

Sample status	Sample (No.)	First run[a] (AU)	Second run[b] (AU)	Change (AU)
WBD-contaminated lime[d]	Lime 1	687.3 [c]	555.7	- 131.6
	Lime 2	684	628.7	- 55.3
	Lime 3	737	681	- 56
	Lime 4	643.7	584.3	- 59.4
	Lime 5	687.3	639	- 48.3
	Lime 6	737	665.7	- 71.3
	Lime 7	643.7	582.7	- 61
	Lime 8	641.7	548.7	- 93
	Lime 9	675	621.7	- 53.3
	Lime 10	637.3	593.7	- 43.6
	Lime 11	641.7	597	- 44.7
	Lime 12	675	632.3	- 42.7
	Lime 13	637.3	572.3	- 65
	Lime 14	643.7	589	- 54.7
	Lime 15	645.3	561.3	- 84
	Lime 16	687.3	645.7	- 41.6
	Lime 17	644.3	570.3	- 74
	Lime 18	647	586	- 61
	Lime 19	663.3	620.3	- 43
Healthy lime	Lime 20	643.7	640.7	± 3
	Lime 21	663.7	663.3	± 0.4
	Lime 22	737	734.7	± 2.3
	Lime 23	643.7	642	± 1.7
	Lime 24	687.3	686.7	± 0.6
	Lime 25	684	683.3	± 0.7
	Lime 26	737	736	± 1
	Lime 27	657.3	656.7	± 0.6

[a]First run at 580 nm [buffer + (QDs-Ab) + (rhodamine-IMP)]
[b]Second run at 580 nm [buffer + (QDs-Ab) + (rhodamine-IMP) + sample]
[c]Each measurement is the average of three replicates
[d]The baseline shift (40 AU) associated with the determined detection limit (5 phytoplasma/µl) has been used as a criterion to decide whether a sample is WBD-contaminated.

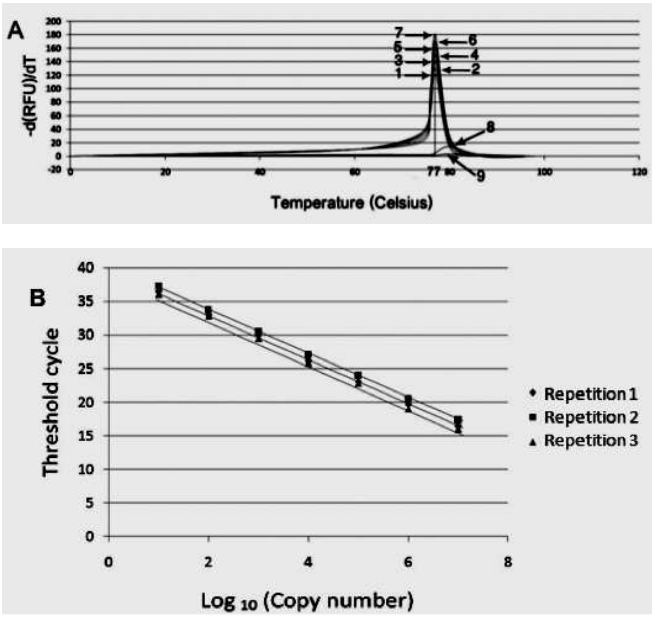

Fig. 5. Specifity of the real time-PCR (IMP3-F/IMP3-R primers) for detection and quantification of phytoplasma associated with WBDL. A. Measured melting curves. A single peak was observed at 77°C for serial dilutions from 10^1 to 10^7 (No. 1-7), whereas primer-dimer accumulation was observed for the healthy plants (No. 8) at 80°C. The DNA-free water control did not show any peak (No. 9). B. Real time PCR calibration curve. Correlation of the threshold cycle (Ct) to the logarithm of the IMP gene copy number obtained with three repetitions of 10-fold serial dilutions of the IMP gene.

ACKNOWLEDGEMENTS

We appreciate the financial support provided by the Agriculture Biotechnology Research Institute of Iran (ABRII). The authors would like to thank Dr. S. Ataei, S. Pahlavan, S. Soheilivand, R. Karami, M. Mesbah, M. Norouzi, A. Rahmani and M. Palizi for their valuable assistance.

REFERENCES

Algar W.R., Krull U.J., 2007. Towards multi-colour strategies for the detection of oligonucleotide hybridization using quantum dots as energy donors in fluorescence resonance energy transfer (FRET). *Journal of Analytica Chimica Acta* **581**(2): 193-201.

Algar W.R., Krull U.J., 2008. Quantum dots as donors in fluorescence resonance energy transfer for the bioanalysis of nucleic acids, proteins, and other biological molecules *Analytical and Bioanalytical Chemistry* **391**: 1609-1618.

Algar W.R, Tavares A., Krull U., 2010. A review of the application of quantum dots as integrated components of assays, bioprobes, and biosensors utilizing optical transduction. *Journal of Analytica Chimica Acta* **673**: 1-25.

Askari N., Salehi Jouzani Gh. R., Mousivand M., Foroutan A., Hagh Nazari A., Abbasalizadeh S., Soheilivand S., Mardi M., 2011. Evaluation of anti-phytoplasma properties of surfactin and tetracycline towards lime witches' broom disease using real-time PCR. *Microbiology and Biotechnology* **21**: 81-88.

Bové J.M., 1986. Outbreaks and new records. Oman. Witches' broom disease of lime. *FAO Plant Protection Bulletin* **34**: 217-218.

Bové J.M., Danet L., Bananej K., Hassanzadeh N., Taghizadeh M., Salehi M., Garnier M., 2000. Witches' broom disease of lime (WBDL) in Iran. *Proceedings of the 14th Conference of the International Organization of Citrus Virologists*: 207-212.

Deng S., Hiruki C., 1991. Amplification of 16S rRNA genes from culturable and nonculturable Mollicutes. *Microbiological Methods* **14**: 53-61.

Frasco M.F., Chaniotakis N., 2009. Semiconductor quantum dots in chemical sensors and biosensors. *Journal of Sensors* **9**: 7266-7286.

Goldman E.R., Balighian E., Kuno M., Labrenz S., Tran P., Anderson G., Mauro J., Mattoussi H., 2002a. Luminescent Quantum Dot-Adaptor Protein-Antibody, Conjugates for Use in Fluoroimmunoassays. *Physica Status Solidi* **229**: 407-414.

Goldman E.R., Balighian E., Mattoussi H., Kuno M., Mauro J., Tran P., Anderson G., 2002b. Avidin: a natural bridge for quantum dot-antibody conjugates. *American Chemical Society* **124**: 6378-638.

Goldman E.R., Mattoussi H., Anderson P., Medintz I., Mauro M., 2005. Fluoroimmunoassays using antibody-conjugate quantum dots. *Methods in Molecular Biology* **303**: 19-34.

Gupta P.D., Dave M., Vasavada A.R., 2005. Protein nanotechnology-A Powerful futuristic diagnosti technique. *Clinical Biochemistry* **20**: 48-53.

Ho Y.P., Chen H.H., Leong K.W., Wang T.H., 2009. Combining QD-FRET and Microfluidics to Monitor DNA Nanocomplex Self-Assembly in Real-Time. *Journal of Visualized Experiments* **30**: 37-42.

Kim K.S., Lee H.S., Yang J.A., Jo M.H., Hahn S.K., 2009. The fabrication, characterization and application of aptamer-functionalized Si-nanowire FET biosensors. *Journal of Nanotechnology* **20**: 223-229.

Lee I.M., Gundersen D.E., Bertaccini A., 1998. Phytoplasma: Ecology and genomic diversity. *Phytopathology* **88**: 1359-1366.

Liu T.C., Zhang H.L., Wang J.H., Wang H.Q., Zhang Z.H., Hua X.F., Cao Y.C., Luo Q.M., Zhao Y.D., 2008. Study on molecular interactions between proteins on live cell membranes using quantum dot-based fluorescence resonance energy transfer. *Analytical and Bioanalytical Chemistry* **391**: 2819-2824.

Medintz I., Clapp A., Mattoussi H., Goldman E.R., Fisher B., Maouro J.M., 2003. Self-assembled nanoscale biosensors based on quantum dot FRET donors. *Nature Materials* **2**: 630-638.

Safarnejad M.R., Salehi-Jouzani G.R., Tabatabaie, Richard M., Twyman M., Schillberg S., 2011. Antibody-mediated resistance against plant pathogens. *Biotechnology Advances* **29**: 961-971.

Shahryari F., Safarnajad M.R., Shams-Bakhsh M., Jouzani G.I., 2010. Toward immunomodulation of witches broom disease of lime (WBDL) by targeting immunodominant membrane protein (IMP) of *Candidatus* Phytoplasma aurantifolia. *Communication in Agriculture and Applied Biological Science* **75**: 789-797.

Shahryari F., Safarnajad M.R., Shams-Bakhsh M., Ataiee S., 2011. Use of a recombinant protein for development of a DAS-ELISA serological kit for sensitive detection of witches' broom disease of lime. *Bulletin of Insectology* **64**: S43-S44.

Shi C.G., Xu J.J., Chen H.Y., 2007. Electrogenerated chemiluminescence and electrochemical bi-functional sensors for H_2O_2 based on CdS nanocrystals/hemoglobin multilayers. *Journal of Electroanalytical Chemistry* **610**: 186-192.

Tang Z., Mallikaratchy P., Yang R., Kim Y., Zhu Z., Wang H., Tan W., 2008. Aptamer Switch Probe Based on Intramolecular Displacement. *American Chemical Society* **130**: 11268-11269.

Whelan J.A., Russell N.B., Whelan M.A., 2003. A method for the absolute quantification of cDNA using real-time PCR. *Immunological Methods* **278**: 261-269.

Youn H.J., Terpetschnig E., Szmacinski H., Lakowicz J.R., 1995. Fluorescence energy transfer immunoassay based on a long-lifetime luminescent metal-ligand complex. *Analytical Biochemistry* **232**: 24-30.

Zamharir M., Mardi M., Alavi M., Hasanzadeh N., Khayam Nekouei M., Zamanizadeh H.R., Alizadeh A.H., Salekdeh Gh., 2011. Identification of genes differentially expressed during interaction of Mexican lime tree infected with "*Candidatus* Phytoplasma aurantifolia. *BMC Microbiology* **11**: 2-9.

Zhang Ch., Johnson L., 2006. Quantum-Dot-Based Nanosensor for RRE IIB RNAΔRev Peptide Interaction Assay. *American Chemical Society* **128**: 5324-5325.

Zhang F., Ali Z., Amin F., Riedinger A., Parak W.J., 2010. In vitro and intracellular sensing by using the photoluminescence of quantum dots. *Analytical and Bioanalytical Chemistry* **397**: 935-942.

Zhang Y.P., Uyemoto J.K., Kirkpatrick B.C., 1998. A small-scale procedure for extracting nucleic acids from woody plants infected with various phytoplasmas for PCR assay. *Journal of Virological Methods* **71**: 45-50.

Zhou M., Ghosh I., 2006. A bright future together. *Peptide Science* **88**: 325-339.

Zreik L., Carle P., Bové J.M., Garnier M., 1995. Characterization of the mycoplasmalike organism associated with witches-broom disease of lime and proposition of a Candidatus taxon for the organism, *Candidatus* Phytoplasma aurantifolia. *International Journal of Systematic Bacteriology* **45**: 449-453.

Received October 11, 2011
Accepted June 25, 2012